ARTICLE | Article in Press

Comparative diagnostic performance of three dimensional transvaginal sonography and three dimensional saline infusion sonohysterography for cesarean scar defects

Atiyeh Najafi · Firoozeh Ahmadi · Ameneh Saadat Varnosfaderani · Samira Vesali · Atefeh Omrani

Received: 30 November 2025 / Accepted: 14 September 2026

Abstract

Cesarean scar defects (CSDs) are disruptions in the myometrium at the site of a previous cesarean delivery and have become a concern in reproductive medicine due to their impact on gynecological and reproductive health. This cross-sectional study compared the diagnostic performance of three-dimensional transvaginal sonography (3D-TVS) and three-dimensional saline infusion sonohysterography (3D-SIS) in detecting CSDs among 403 women with prior cesarean delivery. The primary outcome was the prevalence of CSDs detected by 3D-TVS and 3D-SIS. Secondary outcomes included diagnostic agreement and the correlation of morphological parameters including defect length, width, residual myometrial thickness (RMT), and adjacent myometrial thickness (AMT). CSD prevalence was 34.0% by 3D-TVS and 80.6% by 3D-SIS, demonstrating poor agreement ($\kappa = 0.20$). Sensitivity and specificity of 3D-TVS were 42.15 and 100%, respectively. Measurements from both modalities were positively correlated ($p < 0.0001$), showing strong correlation for RMT ($r = 0.60$) and moderate correlations for defect length ($r = 0.47$), width ($r = 0.57$), and AMT ($r = 0.49$). These findings support a streamlined diagnostic approach: when CSD is detected by 3D-TVS, further 3D-SIS evaluation is likely unnecessary, whereas a negative 3D-TVS finding in symptomatic patients may warrant subsequent 3D-SIS assessment to reduce the risk of missed diagnoses.

Keywords Cesarean scar defect · Isthmocele · Transvaginal sonography · Sonohysterography · Three-dimensional imaging

Abbreviations

CSD	Cesarean scar defects
3D-TVS	Three-dimensional transvaginal sonography
3D-SIS	Three-dimensional saline-infused sonohysterography
RMT	Residual muscle thickness

https://doi.org/10.1038/s41598-026-71975-4

Published online: 19 September 2026

AMT Adjacent myometrial thickness
CS Cesarean section

Introduction

Cesarean delivery rates continue to increase globally, currently exceeding 21% of all births and projected to reach 29% by 2030[1]. Alongside this increase, cesarean scar defect (CSD)—also known as a niche, isthmocele, uterine scar diverticulum, or cesarean scar pouch— has emerged as a recognized long-term complication of cesarean delivery[2–5]. CSD is defined as a myometrial indentation of at least 2 mm at the site of a previous cesarean scar[5]. These defects may vary considerably in their number, shape, and dimensions[6]. The reported prevalence of CSD ranges from 19% to 84%, largely depending on the diagnostic modality used[7]. While often asymptomatic, CSDs may be associated with abnormal uterine bleeding, chronic pelvic pain, dysmenorrhea, secondary infertility, and scar ectopic pregnancy[8]. Accurate characterization is essential to prevent overtreatment and unnecessary surgery. Furthermore, assessing defect morphology and residual myometrial thickness (RMT), regardless of symptoms, is critical to predict and prevent adverse outcomes in future pregnancies[7].

Various modalities are available for evaluating CSD, including two- and three-dimensional transvaginal sonography (2D/3D-TVS), saline or gel contrast sonography, magnetic resonance imaging (MRI), hysterosalpingography, and hysteroscopy[6,9]. Hysterosalpingography detects CSD but cannot assess RMT, while MRI provides accurate anatomical characterization[8], but is less accessible and costlier than ultrasound. TVS is commonly used as a first-line modality because it is rapid, minimally invasive, widely available, and relatively inexpensive[10–12]. While conventional ultrasound may miss subtle defects or inaccurately characterize their morphology and RMT, SIS enhances visualization and precision through uterine cavity distension[13]. Despite the widespread use of both techniques, the optimal diagnostic approach and the relative value of TVS versus SIS remain debated. Therefore, this study aimed to determine CSD prevalence and compare the diagnostic performance of 3D-TVS and 3D-SIS in detecting and characterizing these defects.

Methods

Study design and setting

We conducted a cross-sectional, paired diagnostic comparative study with consecutive enrollment at the Imaging Center of Royan Institute (Tehran, Iran) between 14 September 2024 and 9 July 2025. In this paired-comparison design, all included participants underwent both 3D-TVS and 3D-SIS during a single clinical visit to ensure temporal consistency. Consequently, patients acted as their own controls for the evaluation and comparison of cesarean scar defect (CSD) detection rates and morphometric measurements.

The study was conducted in accordance with the Declaration of Helsinki (1975) and its subsequent amendments. Ethical approval was granted by the Ethics Committee of Royan Institute on 10 September 2024 (IR.ACECR.ROYAN.REC.1403.049). All participants provided written informed consent before their enrollment.

Participants and recruitment

Women referred to the Imaging Center of Royan Institute (Tehran, Iran) between 14 September 2024 and 9 July 2025 to undergo SIS were consecutively enrolled in the study if they had a history of cesarean section and met other inclusion criteria. At our institution, all patients routinely undergo TVS before SIS to exclude pregnancy and provide an initial assessment of the uterus and ovaries.

Women aged 18 to 50 years were eligible for inclusion, provided they had a history of a single cesarean section (either elective or emergency). This specific requirement regarding the number of previous cesarean sections was applied to standardize the cohort and eliminate the potential confounding effect of multiple prior hysterotomies on the morphology and detection of cesarean scar defects. Eligibility required a minimum interval of six months since the cesarean delivery[14]. Participants were excluded if they had known uterine anomalies, an intrauterine contraceptive device, multiple uterine fibroids or any fibroid exceeding 3 cm in diameter, severe adenomyosis, extensive pelvic adhesions, cervical stenosis, or a history of cervical cancer, pregnancy detected on sonographic assessment at the time of imaging, or any contraindication to sonohysterography, such as active pelvic inflammatory disease.

A total of 403 eligible patients who attended the Royan Institute Imaging Center for SIS during the study period were enrolled.

Diagnostic procedures

All examinations were performed by a single board-certified radiologist with 25 years of experience in gynecological imaging, ensuring that all measurements and interpretations were conducted in a standardized and consistent manner. Three-dimensional (3D) imaging analysis was performed offline following real-time examination. Post-processing techniques were applied to measure and visualize specific areas of interest, ensuring optimal image quality and diagnostic accuracy.

3D transvaginal ultrasound (3D-TVS)

All 3D-TVS examinations were performed with the patient in the lithotomy position and an empty bladder during the follicular phase. Imaging was conducted using a Samsung WS80 Elite system equipped with an RIC5-9 3D endovaginal probe operating at a frequency of 5-7.5 MHz. The lower uterine segment was examined in the sagittal plane to localize the niche region. Once the area with the maximal surface dimension was localized, quantitative measurements were obtained.

3D saline infusion sonohysterography (3D-SIS)

3D-SIS was performed immediately following 3D-TVS. A sterile vaginal speculum was first inserted, and the cervix was cleaned with a 10% povidone-iodine solution. The uterine cavity was then distended with normal saline using an intrauterine balloon catheter (18–24 Fr; Well Lead Medical Co., Ltd., Guangzhou, China). During SIS, the transvaginal probe was placed in the posterior vaginal fornix to monitor uterine distension while saline was infused. Optimal visualization of the endometrial cavity, typically achieved with 5–10 mL of saline, allowed detailed assessment of endometrial morphology. The volume of saline was tailored by the operator in real time under ultrasound guidance.

Assessments

The CSD is generally visualized as a cone-shaped hypoechoic scar defect with a depth of $\geq$2 mm, featuring a well-defined apex and base. The apex corresponds to the deepest point within the residual myometrium, whereas the base is contiguous with the adjacent endometrial or cervical surface. CSD dimensions were obtained using electronic calipers, as follows:

1. Length: Maximal length of the defect in the sagittal plane, excluding the endometrium.

2. Width: Maximal transverse diameter of the defect in the transverse plane.

3. Residual muscle thickness (RMT(: Minimal thickness from the niche apex to the serosal surface, measured perpendicular to the serosa in the sagittal plane.

4. Adjacent myometrial thickness (AMT(: Myometrial thickness lateral to the niche base, measured perpendicular to the endometrial canal in the sagittal plane[7,15,16] (Figs. 1 and 2).

CSDs were classified as large when the RMT measured ≤ 2.2 mm on TVS or ≤ 2.5 mm on SIS[9]. Additional sonographic parameters, including uterine dimensions, myometrial echotexture, endometrial thickness, ovarian morphology, and uterine position, were also assessed. Furthermore, demographic characteristics such as age, method of conception (spontaneous or via assisted reproductive technology), and history of cesarean section (type and interval since the procedure), were extracted from patient records.

Statistical analysis

Data were analyzed using IBM© SPSS© Statistics version 24 (IBM© Corp., Armonk, NY, USA). Quantitative variables were summarized as mean (M) ± standard deviation (SD), while qualitative variables were presented as frequency and percentage. Agreement between 3D-TVS and 3D-SIS in evaluating CSD was assessed using Cohen kappa test. Interpretation of kappa values was as follows: < 41% indicates poor agreement; 41%-60% indicates moderate agreement; 61%-80% indicates good agreement; and 81%-100% indicates excellent agreement. The diagnostic performance of 3D-TVS in detecting CSD was evaluated by calculating sensitivity, specificity, positive and negative predictive values, positive and negative likelihood ratios and overall accuracy, all reported with 95% confidence intervals (CIs), using MedCalc version 20. The Correlation of length, width, RMT, and AMT parameters obtained by 3D-TVS and 3D-SIS was assessed using Pearson's correlation. Correlation strength was interpreted according to standard biomedical research guidelines: |r| 0.00–0.19, very weak; 0.20–0.39, weak; 0.40–0.59, moderate; 0.60–0.79, strong; and 0.80–1, very strong.

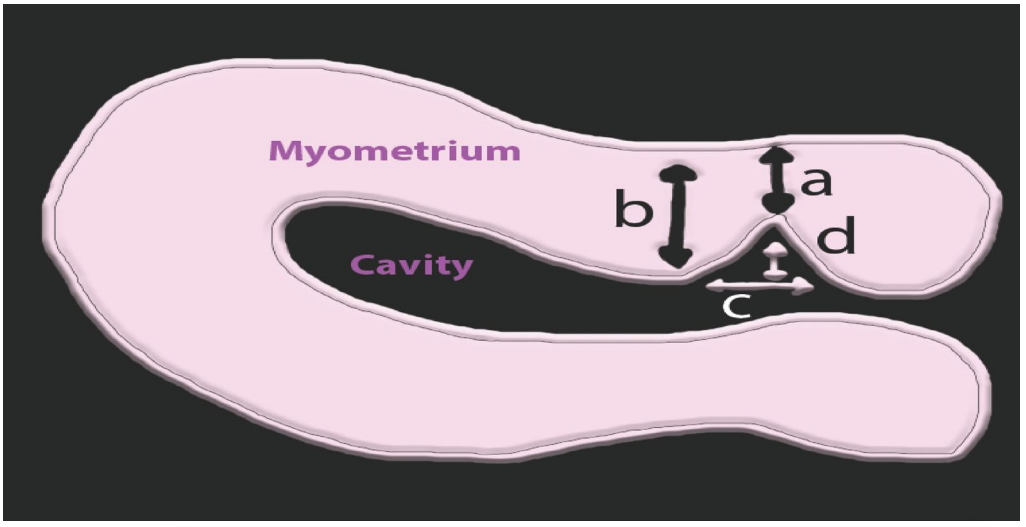

Fig. 1 Schematic representation of CSD measurements: (**a**) Residual myometrium thickness (RMT), (**b**) Adjacent myometrium thickness (AMT), (**c**) width of CSD, (**d**) Length of CSD.

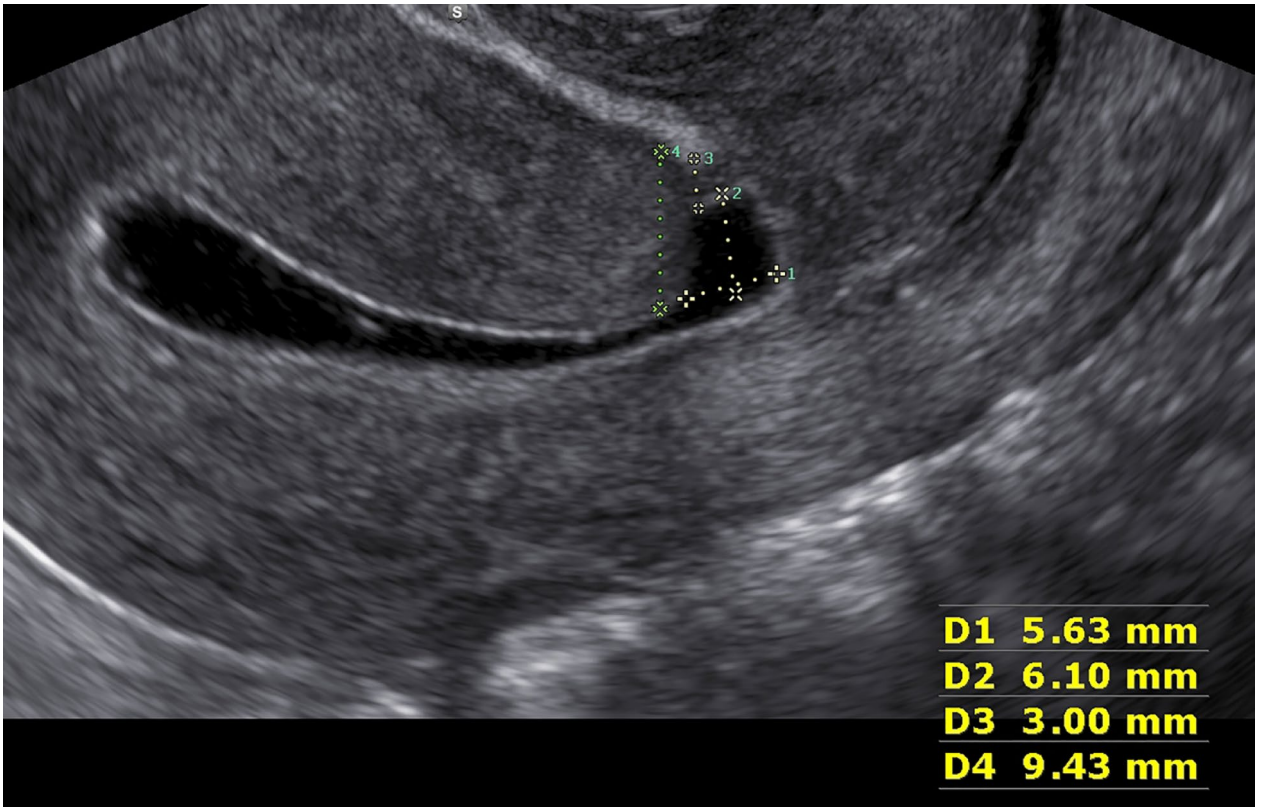

Fig. 2 Ultrasonographic view of CSD measurements: (1) width of CSD, (2) Length of CSD, (3) Residual myometrium thickness (RMT), (4) Adjacent myometrium thickness (AMT).

Results

During the study period, a total of 403 women were recruited, with a mean age of 36.15 ± 4.68 years. Over 90% had a normal uterine size, and 86% had normal ovarian morphology. A retroverted uterus position was observed in 13.9% of the women, while 60% exhibited a heterogeneous uterus echo. More than 50% conceived spontaneously, and the majority) > 70%) of cesarean deliveries were elective (Table 1).

For CSD detection, Cohen's kappa indicated poor agreement between 3D-TVS and 3D-SIS (kappa = 20%) (Fig. 3). Subgroup analyses also showed poor inter-modality agreement: in women with a retroverted uterus (kappa = 25.6%), those ≤ 10 years after cesarean section (kappa = 21%), and those > 10 years post-cesarean section (kappa = 17.2%). When classifying CSDs as large or non-large, the agreement between 3D-TVS and 3D-SIS was moderate (kappa = 46.3%) (Table 2).

The prevalence of CSD was 34.0% by 3D-TVS and 80.6% by 3D-SIS, sensitivity and specificity were 42.15% and 100%, respectively, in comparison with 3D-SIS (Table 3). To further characterize the diagnostic discrepancies between the two modalities, we analyzed the 188 CSDs detected by 3D-SIS but missed by 3D-TVS. Based on 3D-SIS measurements, the mean CSD length and width in these cases were 4.56 ± 1.41 mm and 2.80 ± 1.05 mm, respectively. The mean RMT was 4.45 ± 1.58 mm, suggesting that many of the missed defects were relatively small and had comparatively preserved residual myometrium.

The mean CSD measurements obtained by 3D-TVS were as follows: length 4.00 ± 1.72 mm, width 3.19 ± 1.33 mm, RMT 3.34 ± 1.35 mm, and AMT 8.64 ± 1.89 mm. Corresponding measurements by 3D-SIS were length 4.94 ± 1.68 mm, width 3.23 ± 1.43 mm, RMT 4.03 ± 1.57 mm, and AMT 8.02 ± 1.77 mm. Analysis of these CSD parameters revealed statistically significant positive correlations between 3D-TVS and 3D-SIS for all four variables ($p < 0.0001$), with the strongest correlation observed for RMT ($r = 0.60$) (Table 4).

Table 1 Demographic and clinical characteristics of participants ($n=403$).

Variables		Mean ± SD/*n* (%)
Age (year)		36.15 ± 4.68
Type of caesarean	Elective	289 (71.9%)
	Emergency	113 (28.1%)
CS-US Interval (year)*		7.58 ± 4.07
Pregnancy history	Normal	216 (53.7%)
	Assisted reproductive	186 (46.3%)
Uterus size	Normal	397 (98.5%)
	Abnormal) Top normal due to adenomyosis(	6 (1.5%)
Uterus echo	Normal	158 (39.2%)
	Heterogeneous	245 (60.8%)
Endometrium thickness (mm)		6.83 ± 1.74
Ovary view	Normal	345 (86%)
	Abnormal	56 (14%)
Uterine position	Anteverted	347 (86.1%)
	Retroverted	56 (13.9%)
Ultrasound Date in LMP (Day)**		9.5 ± 1.30

*Cesarean section to ultrasound interval. **Last menstrual period.

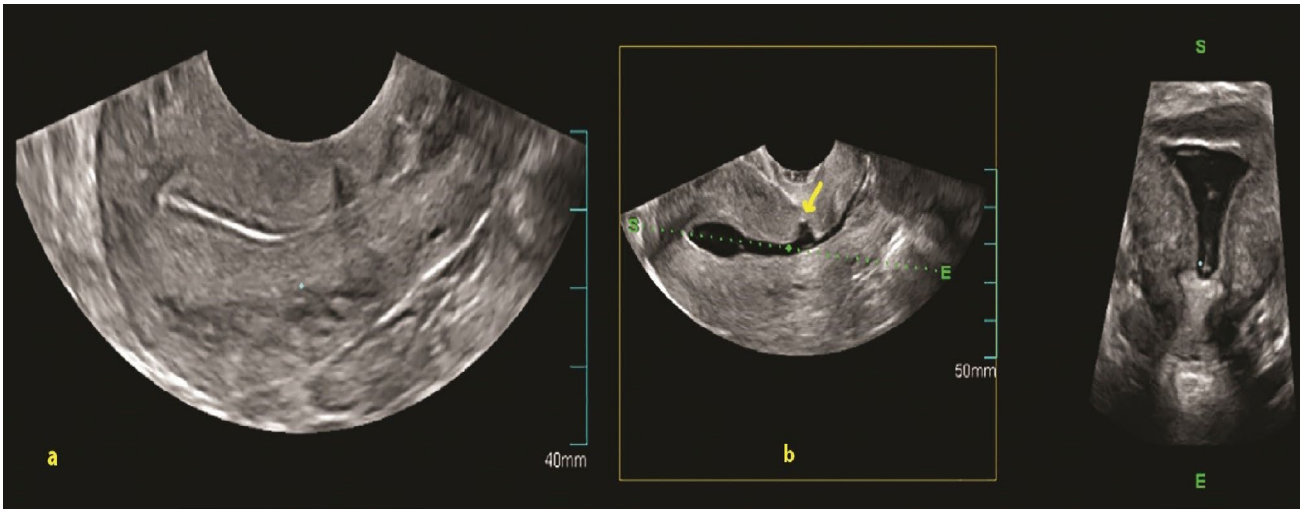

Fig. 3 Comparison of 3D transvaginal ultrasound (3D-TVS) and 3D saline infusion sonohysterography (3D-SIS) for imaging the uterine cesarean scar defect (CSD). (**a**) 3D-TVS image where the CSD is not clearly identifiable. (**b**) 3D-SIS image of the same patient following saline infusion. The distension of the uterine cavity provides contrast, allowing the CSD (arrow) to become clearly delineated and measurable.

Discussion

CSDs are increasingly recognized as a potential factor contributing to secondary infertility, and surgical repair, specially hysteroscopic correction in women with sufficient RMT has shown promise in improving reproductive outcomes[17–19]. Accordingly, accurate diagnosis is a critical first step in identifying suitable candidates for intervention. In this context, our cross-sectional study aimed to compare the diagnostic performance of 3D-TVS and 3D-SIS in the assessment and characterization of CSDs. The prevalence of CSD in our population was 34.0% by 3D-TVS and 80.6% by 3D-SIS. According to Anu et al., the reported prevalence of CSD ranges from 24 to 70% with TVS and 56–84% with SIS[20]. Van der Voet et al. reported a prevalence of 49.6% with TVS and 64.5% with SIS when examinations were conducted 6–12 weeks after cesarean delivery[21]. We conducted evaluations

Table 2 Diagnostic agreement of 3D-SIS and 3D-TVS for CSD evaluation.

a) Inter-modality agreement for CSD diagnosis among all participants.				
3D-SIS	3D-TVS		P-value	Kappa
	Yes	*No*		
Yes	137 (42.2%)	188 (57.8%)	<0.0001	20%
No	0 (0.0%)*	78 (100%)		
b) Inter-modality agreement between 3D-TVS and 3D-SIS for CSD diagnosis in women with a retroverted uterus.				
3D-SIS	3D-TVS		P-value	Kappa
	Yes	*No*		
Yes	21(46.7%)	24 (53.3%)	0.004	25.6%
No	0(0.0%)	11 (100%)		
c) Inter-modality agreement between 3D-TVS and 3D-SIS for CSD diagnosis in participants ≤ 10 years post–cesarean section.				
3D-SIS	3D-TVS		P-value	Kappa
	Yes	*No*		
Yes	99 (40.6%)	145 (59.4%)	<0.0001	21%
No	0 (0%)	67 (100%)		
d) Inter-modality agreement between 3D-TVS and 3D-SIS for CSD diagnosis in participants > 10 years after cesarean section.				
3D-SIS	3D-TVS		P-value	Kappa
	Yes	*No*		
Yes	37 (46.3%)	43 (53.8%)	<0.0003	17.2%
No	0 (0.0%)	11 (100%)		
e) Inter-modality agreement in classifying CSDs as large (RMT < 2.2 mm for 3D-TVS and < 2.5 mm for 3D-SIS) or non-large.				
3D-SIS	3D-TVS		P-value	Kappa
	Large	Non-large		
Large	17 (50%)	17 (50%)	<0.0001	46.3%
Non-large	8 (7.8%)	95 (92.2%)		

*miss diagnosis.

Table 3 Diagnostic performance of 3D-TVS compared with 3D-SIS in CSD detection.

	Sensitivity	Specificity	Positive likelihood ratio	Negative likelihood ratio	Positive predictive value	Negative predictive value	Accuracy
CSD detection	42.15% (36.72% to 47.73%)	100% (95.38% to 100%)	16.44 (4.16 to 64.95)	0.58 (0.53 to 0.63)	100% (97.34% to 100%)	29.32% (27.44% to 31.28%)	53.35% (48.35% to 58.30%)
CSD detection in a retroverted uterus	46.67% (31.66% to 62.13%)	100.00% (71.51% to 100.00%)	-	0.53 (0.41 to 0.70)	100.00% (83.89% to 100.00%)	31.43% (25.86% to 37.59%)	57.14% (43.22% to 70.29%)
Diagnosis of CSD based on time since cesarean delivery ≤ 10 years	40.57% (34.36% to 47.02%)	100% (94.64% to 100%)	1.53 (1.05 to 2.25)	0.59 (0.54 to 0.66)	100% (96.34% to 100%)	31.62% (29.41% to 33.89%)	53.38% (47.66% to 59.03%)
Diagnosis of CSD based on time since cesarean delivery > 10 years	46.25% (35.03% to 57.76%)	100.00% (71.51% to 100.00%)	-	0.54 (0.44 to 0.66)	100.00% (90.51% to 100.00%)	20.37% (17.27% to 23.87%)	52.75% (42.00% to 63.31%)
CSD classification as large	50% (32.43% to 67.57%)	92.23% (85.27% to 96.59%)	6.44 (3.05 to 13.57)	0.54 (0.39 to 0.76)	68.00% (50.20% to 81.75%)	84.82% (79.90% to 88.71%)	81.75% (74.25% to 87.83%)

Confidence interval (CI: lower to upper).

no earlier than six months after cesarean section, as the wound-healing process is reported to take at least this duration[22].

Our findings indicate poor agreement between 3D-TVS and 3D-SIS in detecting CSD (Cohen's kappa = 0.20, $p < 0.001$). 3D-TVS fails to detect over half of CSDs. Therefore, when exclusion of CSD is clinically important,

Table 4 Correlation between 3D-SIS and 3D-TVS in sonographic characteristics of CSD (mm).

	Minimum	Maximum	Mean ± Standard deviation (SD)		Correlation coefficient
3D-TVS* CSD length	1.0	15.0	4.00	1.72	$r=0.47$
3D-SIS** CSD length	1.5	14.0	4.94	1.68	$P<0.0001$
3D-TVS CSD width	1.0	10.7	3.19	1.33	$r=0.57$
3D-SIS CSD width	1.3	10.0	3.23	1.43	$P<0.0001$
3D-TVS RMT***	1.0	9.0	3.34	1.35	$r=0.60$
3D-SIS RMT	1.0	10.0	4.03	1.57	$P<0.0001$
3D-TVS AMT****	2.9	15.0	8.64	1.89	$r=0.49$
3D-SIS AMT	4.0	16.0	8.02	1.77	$P<0.0001$

*Three-Dimensional Transvaginal Sonography-**Three-Dimensional Saline Infusion Sonohysterography -***Residual Myometrial Thickness-****Adjacent Myometrial Thickness.

especially in symptomatic patients, a negative 3D-TVS result should not be considered definitive, and further evaluation with 3D-SIS may be warranted. Analysis of the CSDs detected by 3D-SIS but missed by 3D-TVS helps explain the observed diagnostic discrepancy. In general, these missed defects tended to be relatively small and were often associated with comparatively preserved residual myometrium, which may make them less conspicuous on non-distended 3D-TVS images. Beyond the small morphometric dimensions, the presence of blood clots or mucus retained within the CSD represents another critical confounding factor. On conventional 3D-TVS, these clots can act as an acoustic barrier or mimic normal myometrium, thereby masking the defect. Conversely, the saline distension during 3D-SIS actively flushes and displaces these intra-defect materials, enhancing the contrast and visibility of the defect[23]. Consistent with our findings, Antila-Långsjö et al.[10] recommended SIS as the preferred diagnostic method for CSD, noting that TVS alone may underestimate its prevalence. Similarly, Ahmed et al.[24] demonstrated the superiority of SIS over TVS in assessing CSD and suggested that combining both modalities could reduce the need for hysteroscopy.

The higher detection rate of 3D-SIS observed in the present study should be interpreted in the context of both saline-induced uterine cavity distension and three-dimensional image reconstruction. Saline infusion may improve the visualization of subtle or shallow defects by outlining the CSD and separating its margins from the surrounding myometrium, whereas three-dimensional imaging enables multiplanar assessment and may facilitate more comprehensive characterization of CSD morphology, particularly its width and RMT[5,25]. In a comparative study of 2D-SIS and 3D-SIS, agreement between the two techniques was high for CSD length but lower for RMT and CSD width, suggesting that three-dimensional reconstruction may provide additional information for selected morphometric parameters, especially those better assessed in planes other than the conventional sagittal view[25]. However, the European Niche Taskforce recommends assessment of the CSD in at least the sagittal and transverse planes and does not consider three-dimensional imaging or the coronal plane mandatory for standard evaluation[5]. Thus, the diagnostic advantage of 3D-SIS over 3D-TVS in our study cannot be attributed solely to the three-dimensional technique. Rather, it likely reflects the combined contribution of saline-induced cavity distension and multiplanar image assessment.

This comparative analysis of CSD morphometric measurements between 3D-TVS and 3D-SIS demonstrated statistically significant, moderate-to-strong positive correlations for all parameters: length (r = 0.47), width (r = 0.57), RMT (r = 0.60), and AMT (r = 0.49) (all $p < 0.0001$). These results indicate a consistent relationship between the measurements obtained by the two techniques. Similarly, Rasheedy et al.[13] reported strong correlations between TVS and SIS for assessing CSD parameters, including length (r = 0.81), width (r = 0.95), RMT (r = 0.91), and AMT (r = 1.00).

In line with the study by Anter et al.[26], our findings showed 3D-SIS identified a greater number of defects as large compared to 3D-TVS. This discrepancy may arise from the capacity of 3D-SIS to distend the scar niche[23], which results in thinner RMT measurements and, consequently, a higher proportion of defects being classified

as large compared with 3D-TVS. The tendency of 3D-SIS to classify more defects as large should therefore be interpreted as a technical measurement-related effect rather than a true increase in defect size.

Beyond identifying CSDs, accurate characterization of their morphology may contribute to therapeutic decision making. In symptomatic women, the choice of management should be individualized according to symptom severity, reproductive intentions, RMT, and defect morphology[3,5]. RMT is particularly relevant when selecting the surgical route, as hysteroscopic niche resection has generally been evaluated in women with sufficient residual myometrium, commonly considered to be an RMT of approximately 3 mm or greater, whereas a thinner residual myometrium or more extensive defects may favor laparoscopic or transvaginal repair[3,27]. In the present study, although 3D-SIS detected substantially more CSDs than 3D-TVS, morphometric measurements, including both RMT and AMT, showed moderate-to-strong correlations between the two modalities among defects visualized by both techniques. Therefore, when a CSD is clearly identified on 3D-TVS, this modality may provide sufficiently reliable morphometric information for initial clinical assessment and may not necessitate additional 3D-SIS solely for dimensional evaluation. Conversely, because a negative 3D-TVS examination does not reliably exclude CSD, 3D-SIS may be particularly useful in symptomatic women or in those with persistent clinical suspicion despite negative or inconclusive 3D-TVS findings. Nevertheless, as treatment allocation and postoperative outcomes were not assessed in our study, the role of either modality in improving treatment selection requires confirmation in prospective outcome-based studies.

To the best of our knowledge, this is the first study to compare 3D-TVS and 3D-SIS for the detection of CSD. The three-dimensional imaging technique offers volumetric data that can be analyzed offline, allowing for a more precise and comprehensive evaluation of CSD morphology. A strength of this study is that all participants underwent both 3D-TVS and 3D-SIS during the same visit, ensuring consistency in procedural conditions and menstrual cycle timing. Moreover, the study included a relatively large sample size, which strengthens the reliability and enhances the generalizability of the findings. A limitation of this study is that both examinations were performed in the same visit by the same investigator without masking between the 3D-TVS and 3D-SIS interpretations. However, this approach reflects routine clinical practice, where assessments are commonly conducted sequentially by the same physician. Consequently, the risk of significant bias was likely attenuated, as 3D-TVS—performed first—demonstrated a lower prevalence of CSD, thereby reducing the likelihood of observer bias during the subsequent 3D-SIS evaluation. Moreover, the diagnostic accuracy of sonographic evaluations is inherently dependent on the technical specifications of the ultrasound equipment and the professional expertise of the operator. These operator-dependent and equipment-related factors may limit the generalizability of the findings.

We recommend that future multi-center studies, including more diverse populations in terms of age, number of prior cesarean deliveries, symptomatology, and uterine morphology, be conducted to enhance the generalizability of results.

Conclusion

In summary, the findings of this study suggest that a two-tiered diagnostic strategy could be considered for the evaluation of CSD. In cases where a CSD is clearly visualized on 3D-TVS, direct progression to clinical management may be reasonable, without routine use of additional imaging modalities for confirmation or detailed morphometric assessment. However, a negative 3D-TVS finding should be interpreted with caution in symptomatic patients. In such cases, further evaluation with 3D-SIS may provide additional diagnostic information and help reduce the risk of missed CSD.

Overall, this approach promotes more efficient use of clinical resources by reserving the more complex, gold-standard modality (3D-SIS) for cases in which initial ultrasound findings are inconclusive, while still ensuring accurate and reliable diagnosis.

Acknowledgements The authors sincerely thank the colleagues in the Imaging Department at the Royan Research Institute

for their valuable support in sample preparation and imaging procedures.

Author contributions A.N. and F.A. contributed to the conception and design of the study; A.N. did the literature search; F.A. carried out the image acquisition and analysis; A.S.V. curated the data; S.V. performed the statistical analysis; A.N., F.A., and A.O. wrote the first draft of the manuscript. All authors contributed to the manuscript revision and read and approved the submitted version.

Data availability The datasets used and/or analyzed during the current study are available upon reasonable request from the corresponding author, Dr. Firoozeh Ahmadi (Dr.Ahmadi1390@gmail.com).

Declarations

Competing interests The authors declare no competing interests.

References

1. World Health Organization. Caesarean section rates continue to rise, amid growing inequalities in access. https://www.who.int/news/item/16-06-2021-caesarean-section-rates-continue-to-rise-amid-growing-inequalities-in-access (2021).
2. Bi, B. et al. Analysis on clinical association of uterine scar diverticulum with subsequent infertility in patients underwent cesarean section. *Medicine* **100** (41), e27531 (2021).
3. Dominguez, J. A. et al. Diagnosis and management of isthmocele (Cesarean scar defect): a SWOT analysis. *Ultrasound Obstet. Gynecol.* **62** (3), 336–344 (2023).
4. Fakhr, M. S. et al. Investigating the risk factors for isthmocele development after cesarean delivery. *AJOG global Rep.* **4** (2), 100299 (2024).
5. Jordans, I. P. M. et al. Sonographic examination of uterine niche in non-pregnant women: a modified Delphi procedure. *Ultrasound Obstet. Gynecol.* **53** (1), 107–115 (2019).
6. Armstrong, F. et al. Cesarean scar niche: An evolving concern in clinical practice. *Int. J. Gynaecol. Obstet.* **161** (2), 356–366 (2023).
7. Verberkt, C. et al. How to perform standardized sonographic examination of uterine niche in non-pregnant women. *Ultrasound Obstet. Gynecol.* **60** (3), 420–424 (2022).
8. Kremer, T. G., Ghiorzi, I. B. & Dibi, R. P. Isthmocele: an overview of diagnosis and treatment. *Revista da Associacao Med. Brasileira (1992)*. **65** (5), 714–721 (2019).
9. Lin, P. L., Hou, J. H. & Chen, C. H. A common problem between gynecology, obstetrics, and reproductive medicine: Cesarean section scar defect. *Taiwan. J. Obstet. Gynecol.* **63** (4), 459–470 (2024).
10. Antila-Långsjö, R., Mäenpää, J. U., Huhtala, H., Tomás, E. & Staff, S. Comparison of transvaginal ultrasound and saline contrast sonohysterography in evaluation of cesarean scar defect: a prospective cohort study. *Acta Obstet. Gynecol. Scand.* **97** (9), 1130–1136 (2018).
11. Zhou, X., Zhang, T., Qiao, H., Zhang, Y. & Wang, X. Evaluation of uterine scar healing by transvaginal ultrasound in 607 nonpregnant women with a history of cesarean section. *BMC Women's Health*. **21** (1), 199 (2021).
12. Allameh, Z. et al. A transvaginal ultrasound-based diagnostic calculator for uterus post-cesarean scar defect. *BMC Women's Health*. **23** (1), 558 (2023).
13. Rasheedy, R., Sammour, H., Elkholy, A. & Fadel, E. Agreement between transvaginal ultrasound and saline contrast sonohysterography in evaluation of cesarean scar defect. *J. Gynecol. Obstet. Hum. Reprod.* **48** (10), 827–831 (2019).
14. Naji, O. et al. Standardized approach for imaging and measuring Cesarean section scars using ultrasonography. *Ultrasound Obstet. Gynecol.* **39** (3), 252–259 (2012).

15. Jiang, Y., Qiao, X., Li, T., Wen, J. & Luo, H. Comparison of ultrasonic diagnosis of cesarean scar defects at different timepoints following cesarean section. *Quant. imaging Med. Surg.* **14** (8), 5490–5498 (2024).
16. Jordans, I. et al. Sonographic examination of uterine niche in non-pregnant women: a modified Delphi procedure. *Ultrasound Obstet. Gynecol.* **53** (1), 107–115 (2019).
17. Harjee, R., Khinda, J. & Bedaiwy, M. A. Reproductive outcomes following surgical management for isthmoceles: A systematic review. *J. Minim. Invasive. Gynecol.* **28** (7), 1291–302e2 (2021).
18. Jayasundara, D., Jayawardane, I., Jayasingha, T. & Weliange, S. Exploring uterine niche: a systemic review on secondary infertility rates, pathophysiological correlations, impact on assisted reproduction technology (ART), and the efficacy of surgical interventions. *BMC Pregnancy Childbirth*. **25** (1), 566 (2025).
19. Vidal, A. et al. High live birth rates after laparoscopic isthmocele repair in infertility: a systematic review and meta-analysis. *Front. Endocrinol.* **16**, 1507482 (2025).
20. Vigashini, A. & Pallavee, P. Prevalence and risk factors of sonographically detected cesarean scar defects: A review. *SBV J. Basic. Clin. Appl. Health Sci.* **7** (3). (2024).
21. van der Voet, L. F., Bij de Vaate, A. M., Veersema, S., Brölmann, H. A. & Huirne, J. A. Long-term complications of caesarean section. The niche in the scar: a prospective cohort study on niche prevalence and its relation to abnormal uterine bleeding. *BJOG: Int. J. Obstet. Gynecol.* **121** (2), 236–244 (2014).
22. Jiang, Y. et al. Comparison of ultrasonic diagnosis of cesarean scar defects at different timepoints following cesarean section. *Quant. imaging Med. Surg.* **14** (8), 5490–5498 (2024).
23. Ahmadi, F., Akhbari, F. & Niknejad, F. Various types of niche imaging by sonohysterography. 30th Iranian Congress of Radiology. *Iranian J. Radiol.* 11 (.2014).
24. Ahmad, M., Mohammed, A., Ali, W., Bahy, R. & Alam-Eldeen, M. Diagnostic yield of transvaginal ultrasonography versus saline: infused sonohysterography in the evaluation of post-cesarean section uterine niche. *J. Ultrasound*. **28** (1), 107–117 (2025).
25. Alalfy, M. et al. Evaluation of the cesarean scar Niche in women with secondary infertility undergoing ICSI using 2D sonohysterography versus 3D sonohysterography and setting a standard criteria; alalfy simple rules for Scar assessment by ultrasound to prevent health problems for women. *Int. J. women's health*. **12**, 965–974 (2020).
26. Anter, M., Gad, M., Fahmy, E. & Al Halaby, A. Endovaginal ultrasound versus hysterosalpingography in evaluation of cesarean scar. *Egypt. J. Hosp. Med.* **82** (4), 773–777 (2021).
27. Vervoort, A. et al. Hysteroscopic resection of a uterine caesarean scar defect (niche) in women with postmenstrual spotting: a randomised controlled trial. *BJOG: Int. J. Obstet. Gynecol.* **125** (3), 326–334 (2018).

Authors and Affiliations

Atiyeh Najafi[1] · Firoozeh Ahmadi[1] · Ameneh Saadat Varnosfaderani[1] · Samira Vesali[2] · Atefeh Omrani[3]

✉ Firoozeh Ahmadi
dr.ahmadi1390@gmail.com

[1] Department of Reproductive Imaging, Reproductive Biomedicine Research Center, Royan Institute for Reproductive Biomedicine, ACECR, Tehran, Iran

[2] Department of Basic and Population Based Studies in NCD, Reproductive Epidemiology Research Center, Royan Institute, ACECR, Tehran, Iran

[3] Faculty of Health Sciences and Wellbeing, School of Nursing and Health Sciences, University of Sunderland in London, London, UK